

RESEARCH ARTICLE

Open Access



miR-196b strictly regulates and reliably predicts the response to cetuximab in colorectal cancer

Shiyun Chen^{1,2†}, Zhaoli Tan^{2†}, Yanli Lin^{1†}, Fang Pang^{1,2,3}, Xiaojie Wu¹, Xiang Li¹, Yumeng Cui¹, Weiling Man¹, Ying Li¹, Yanghua Li¹, Lu Han², Miaomiao Gou², Zhikuan Wang^{2*}, Guanghai Dai^{2*} and Youliang Wang^{1*} 

[†]Shiyun Chen, Zhaoli Tan and Yanli Lin contributed equally to this work.

*Correspondence: wangzkme@sohu.com; daigh301@vip.sina.com; wang_you_liang@aliyun.com

¹ Laboratory of Advanced Biotechnology, Beijing Institute of Biotechnology, Beijing 100071, China

² Department of Oncology, The Fifth Medical Center, Chinese PLA General Hospital, Beijing 100071, China

³ School of Medicine, Nankai University, Tianjin 300071, China

Abstract

Background: Cetuximab resistance severely restricts its effectiveness in the treatment of patients with metastatic colorectal cancer (CRC). Previous studies have predominantly focused on the genetic level, with scant attention to the nongenetic aspects. This study aimed to identify the crucial microRNA (miRNA) that is responsible for cetuximab resistance.

Methods: Key miRNAs were identified using small RNA sequencing analysis. miR-196b's role and mechanism in cetuximab resistance was explored by in vitro and in vivo experiments. Clinical blood samples were dynamically analyzed using droplet digital polymerase chain reaction (PCR) to assess the predictive value of miR-196b for efficacy.

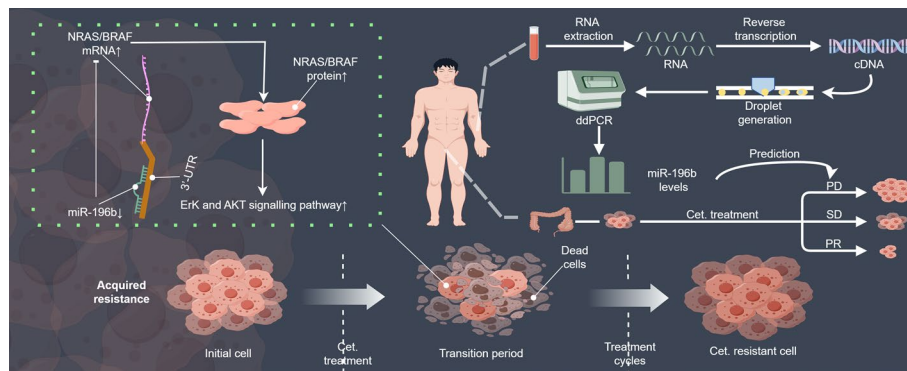
Results: We initially discovered that the extracellular signal-regulated kinase (ERK) signaling pathway was progressively activated during the acquisition of cetuximab resistance in CRC cells. Further study determined that miR-196b can inhibit the activity of ERK and protein kinase B (AKT) signaling pathways by downregulating both NRAS and BRAF, which can kill two birds with one stone, thus enhancing the sensitivity of colorectal cancer cells to cetuximab. The expression of miR-196b was found to be significantly downregulated in both cetuximab-resistant cells and the tumor tissues of patients exhibiting resistance. In the presence of cetuximab, overexpression of miR-196b further inhibited the proliferation and migration and promoted the apoptosis of CRC cells, while miR-196b silencing had the opposite effects. Importantly, analysis of clinical blood samples confirmed that miR-196b can serve as a predictive and dynamic biomarker for monitoring the outcomes of patients with CRC treated with cetuximab.

Conclusions: This study supports that activation of the ERK signaling pathway is a key factor in cetuximab resistance. In addition, miR-196b can modulate and predict the CRC response to cetuximab, holding broad potential applications.

Keywords: Cetuximab resistance, MicroRNA, Colorectal cancer, Prognosis



Graphical Abstract



Background

Colorectal cancer (CRC) is a common malignant tumor. In 2022, its global incidence ranks third and its mortality second among all cancers [1]. As a result, such a high incidence and mortality rate of cancer needs to be taken seriously. Cetuximab, an EGFR monoclonal antibody, represents a significant advancement in treating patients with metastatic CRC (mCRC) and has become the standard therapy for patients with *RAS/RAF* wild-type CRC in stage IV [2]. However, its drug resistance severely limits the clinical results, and rates have reached as high as 70% for patients taking cetuximab therapy within 1 year [3]. Therefore, it is crucial to investigate the mechanisms underlying cetuximab resistance, develop strategies to overcome it, and enhance the prognosis of patients with mCRC, thereby achieving individualized and precise treatment.

Our previous study found that *PRSSI* was strongly associated with cetuximab resistance [4]. Other genes such as *EGFR*, *KRAS*, *NRAS*, *BRAF*, *PIK3 CA*, and *MET* have also been implicated in cetuximab resistance [5–7]. However, these studies focused more on the genetic level and little on the nongenetic level. There is approximately 30% of cetuximab resistance stemming from unknown, apparently nongenetic resistance mechanisms [8]. Over the past decade, advancements in high-throughput transcriptome sequencing technology and bioinformatics methods have enabled researchers to discover the significant role of noncoding RNA (ncRNA) in the development of resistance to epidermal growth factor receptor (EGFR) monoclonal antibodies. This highlights the necessity of exploring nongenetic factors to fully understand and address cetuximab resistance.

MicroRNA (miRNA), a component of ncRNA, mainly regulates target gene expression by participating in posttranscriptional gene regulation [9]. Notably, a single miRNA can simultaneously regulate multiple target mRNAs, thereby influencing multiple signaling pathways. This multifaceted regulation plays a crucial role in tumorigenesis and the development of drug resistance [10–12]. However, the specific impact of miRNAs on resistance to cetuximab remains unclear.

The importance of the extracellular signal-regulated kinase (ERK) signaling pathway in tumor-related studies has been consistently highlighted [6, 13, 14]. In our study, we initially observed that the ERK signaling pathway was progressively upregulated during the development of cetuximab resistance in two CRC cell lines. To investigate the potential upstream regulators, we carried out small RNA sequencing. Our analysis revealed a significant downregulation of miR-196b in both cetuximab-resistant CRC cell models and resistant tissues of patients with mCRC. Fundamental research has demonstrated that miR-196b targets classical resistance genes *NRAS* and *BRAF*, leading to the downregulation of the ERK and protein kinase B (AKT) signaling pathways and restoring cetuximab responsiveness both in vitro and in vivo. More importantly, clinical studies have shown that plasma miR-196b levels can effectively predict and dynamically monitor cetuximab efficacy in patients with mCRC, indicating promising clinical applications.

Methods

Cell culture

This study used three human CRC cell lines, DiFi, LIM1215, and HT-29. HT-29 and LIM1215 were purchased from the American Tissue Culture Collection (ATCC, USA) and WHELAB, respectively. DiFi was provided by Dr. Z. Tan (Beijing Institute of Biotechnology) [4]. Among them, DiFi and LIM1215 were RAS and RAF wild-type cell lines, while HT-29 was a BRAF mutant cell line. All cells were cultured in a sterile humidified incubator at 37 °C with 5% CO₂, and 10% fetal bovine (Gibco, USA) serum was added to all media. DiFi was cultured using Dulbecco's modified Eagle's medium (DMEM; Gibco, USA), while LIM1215 and HT-29 were cultured using 1640 medium (Gibco, USA). In addition, we established two types of CRC-resistant cells, DiFi-R and LIM-R. The highly sensitive cell line DiFi was continuously cultured in a medium containing 10 µg/mL of cetuximab, while the moderately sensitive cell line LIM1215 was continuously cultured in a medium containing 200 µg/mL of cetuximab. During the long-term drug-induced resistance of both two CRC cells, we cryopreserved the cells at all stages. When the half maximal inhibitory concentration (IC₅₀) reached more than ten times that of the parental strain, the drug-resistant model was considered to be successfully constructed.

Construction of stably infected cell lines

To construct cell lines that stably overexpressed or inhibited miR-196b, we used the corresponding lentiviruses to infect designated cells (see Supplementary Material Methods for plasmid profile). All lentiviruses were purchased from GenePharma (Shanghai, China). After a successful lentiviral infection, we used a medium that contained 2 µg/mL of puromycin (Invitrogen, USA) to continuously incubate the cells for more than 4 weeks, after which the puromycin concentration was halved for long-term culture. Similarly, to construct a cell line with stable knockdown of *NRAS*/*BRAF*, we also used lentiviral infection. The cells were then incubated continuously with a medium containing 500 ng/mL of hygromycin (Invitrogen, USA) for more than 4 weeks, and then the hygromycin concentration was halved for long-term culture.

Patient clinicopathologic data and sample collection

Clinicopathologic data and blood specimens were prospectively collected from 97 patients with advanced RAS/RAF wild-type CRC treated with cetuximab at the Chinese PLA General Hospital (see Supplementary Material Methods for details). This study was approved by the Ethics Committee of the Chinese PLA General Hospital (KY2023-6-42-1). Informed consent from each patient was obtained, and the study was conducted following the principles of the Declaration of Helsinki.

Quantitative reverse transcription polymerase chain reaction (qRT-PCR)

Trizol reagent (Invitrogen, USA) was used to extract total RNA from tissues/cells, and a NanoDrop 1000 spectrophotometer was used to measure the RNA concentration. For subsequent miRNA or mRNA detection, RNA was reverse-transcribed into complementary DNA (cDNA) by the Mir-X™ miRNA First Strand Synthesis (Takara, Japan) or the High-Capacity cDNA Reverse Transcription Kit, respectively. The CFX96 Real-Time PCR System (Bio-Rad, USA) and Thunderbird SYBR qPCR Mix (Toyobo, Japan) were adopted to conduct quantitative polymerase chain reaction (qPCR) for amplifying cDNA. Internal references are U6 and glyceraldehyde 3-phosphate dehydrogenase (GAPDH).

Small RNA sequence

Library construction of small RNA was performed using TruSeq Small RNA Library Preparation Kits (Illumina, USA). Then, high-throughput sequencing was performed using Illumina HiSeq™2500.

Cell viability assay

The experiments were conducted using the CellTiter-Glo Luminescent Cell Viability Assay (Promega, USA). According to the manufacturer's instructions, 96-well plates were inoculated with 2×10^3 cells/well. The cells were incubated with a medium containing different concentrations of cetuximab for 72 h after attachment to the wall. Then the CellTiter Glo Reagent was incorporated at the same volume as the medium, mixed on a shaker for 2 min, let stand at room temperature for 10 min, and, finally, luminescence was recorded.

Cell proliferation assay

The BeyoClick™ EdU Cell Proliferation Kit with Alexa Fluor 594 (Reyotime, China) was used to assay the cell proliferation rate, inoculating 8×10^4 cells/well into 4-well slides. After the cells adhere, we added culture medium containing 10 μ M EdU and incubated for 2 h. The experiment was conducted following the manufacturer's instructions, and the counts were monitored under a fluorescence microscope.

Apoptosis detection

Cells were digested from culture flasks and washed with phosphate-buffered saline (PBS). Annexin V-FITC and propyl iodide staining was conducted following the

instructions of the Annexin V-FITC Apoptosis Detection Kit (Beyotime, China). The apoptosis rate was detected using flow cytometry.

Migration and wound-healing assay

A total of 4×10^4 cells were resuspended using serum-free medium and inoculated into the top chamber of 8.0 μm -diameter micropore membranes (Corning, USA). The bottom chamber was placed in a medium with 20% fetal bovine serum. After 24 h of incubation, cells were fixed by ethanol and then stained with 0.1% crystal violet. Before the wound-healing assay, 5×10^5 cells were inoculated into a six-well plate, and the wound line was created manually when the cell density reached about 95%. Cell migration after 48 h was assessed using the wound width at 0 h as a standard.

Dual-luciferase reporter gene analysis

The original/mutated sequences of the 3'UTR of BRAF/NRAS were constructed into pGL3 Luciferase Reporter Vectors (Promega, USA), and these vectors were cotransfected with miR-196b mimics into 293 T cells in 24-well plates. After 48 h transfection, the expression levels of the reporter genes were detected using the Dual-Luciferase Reporter Assay System (Promega, USA).

Western blot

Proteins from cells/CRC tissues were extracted with radioimmunoprecipitation assay buffer (RIPA) lysis buffer (Thermo Scientific, USA). Sodium dodecyl sulfate-polyacrylamide gel electrophoresis (SDS-PAGE) was employed to separate the proteins and transfer them to a polyvinylidene fluoride (PVDF) membrane (Millipore, USA). The membranes were closed with 5% skimmed milk and incubated with primary antibodies (see supplementary methods for details), followed by incubation with the secondary horseradish peroxidase (HRP)-coupled antibody at room temperature for 1 h. Finally, immunoreactive protein complexes were visualized using enhanced chemiluminescence (ECL) detection reagent (PerkinElmer, USA).

Xenograft nude mice experiments

The 4-week-old female nude mice were purchased from GemPharmatech (China) and raised under pathogen-free conditions according to strict standards. Fluorokinase-labeled miR-196b overexpressing/miRCont group of HT-29 cells (2×10^6)/LIM1215 cells (5×10^6) were injected subcutaneously into the right axilla of nude mice. When the average tumor size was approximately 100 mm^3 , mice were randomly assigned to the cetuximab administration group/PBS group. Cetuximab was administered via intraperitoneal injection at a dose of 1 mg per mouse every 3 days. The control group was given sterile PBS in the same manner. Tumor changes were monitored by vernier calipers and the bioluminescence channel of the IVIS Spectrum. After 30 days of observation, the mice were euthanized and tumor tissues were collected. Animal experiments were performed

after approval by the Animal Ethical and Welfare Committee of the Academy of Military Medical Sciences (IACUC-DWZX-2023–052).

Immunohistochemical (IHC) analyses

Paraffin-embedded fixation of xenograft tumor tissues was performed to make sections. According to the manufacturer's instructions, sections were incubated with primary antibodies (see Supplementary Material Methods for details). The cells were then incubated with secondary antibodies, stained with diaminobenzidine (DAB), and counter-stained with hematoxylin for the nuclei.

Droplet digital polymerase chain reaction (ddPCR)

Plasma RNA was reverse transcribed into cDNA by means of the TaqMan™ Micro-RNA Reverse Transcription Kit (Thermo Fisher Scientific, no. 4,366,596, Italy) following the manufacturer's instructions. miR-196b Taqman probe was synthesized by Thermo Fisher Scientific (Italy). The ddPCR reaction system consisted of 10 μ L ddPCR supermix for probes (Bio-Rad, no. 1,863,025, USA), 2.0 μ L cDNA, 1.0 μ L miR-196b probe, and nuclease-free water; the total volume of the reaction system was 20 μ L. ddPCR reactions were carried out using the Automated QX200 droplet digital PCR (ddPCR) system (Bio-Rad, no. 1,864,001, USA).

Statistical analysis

Statistical analysis and visualization were performed using IBM SPSS version 26, Graph-Pad Prism 8 and R version 4.3.0. All experiments conducted in this study were repeated independently at least three times. Data were presented as mean \pm standard error of the mean (SEM). Differences between groups were compared by independent samples *t*-test or two-way analysis of variance (ANOVA). Kaplan–Meier was used to plot survival curves. Meaningful factors, found by univariate Cox analysis and added to multivariate Cox analysis, were used to identify the independent risk factors. Categorical variables were tested using χ^2 or the Fisher exactly. Cutoff values were determined on the basis of receiver operating characteristic (ROC) curve analysis. A *P*-value < 0.05 indicated statistically significant differences.

Results

miR-196b modulates the ERK signaling pathway during cetuximab resistance

A recent important report has highlighted the crucial role of ERK in resistance to KRAS–ERK–MAPK-targeted therapy [6], and both RAS and ERK are downstream components of the EGFR signaling pathway. Building on this understanding, we sought to investigate whether alterations in the ERK signaling pathway occur during the development of cetuximab-acquired resistance. Our results showed that the ERK signaling pathway was activated progressively during the transition from initially sensitive cells (DiFi and LIM1215) to drug-resistant cells (DiFi-R and LIM-R) (Fig. 1A–D).

To investigate the upstream regulators, we conducted small RNA sequencing on two CRC cell models (Fig. 1E) and tumor tissues from two patients with mCRC (Fig. 1F,

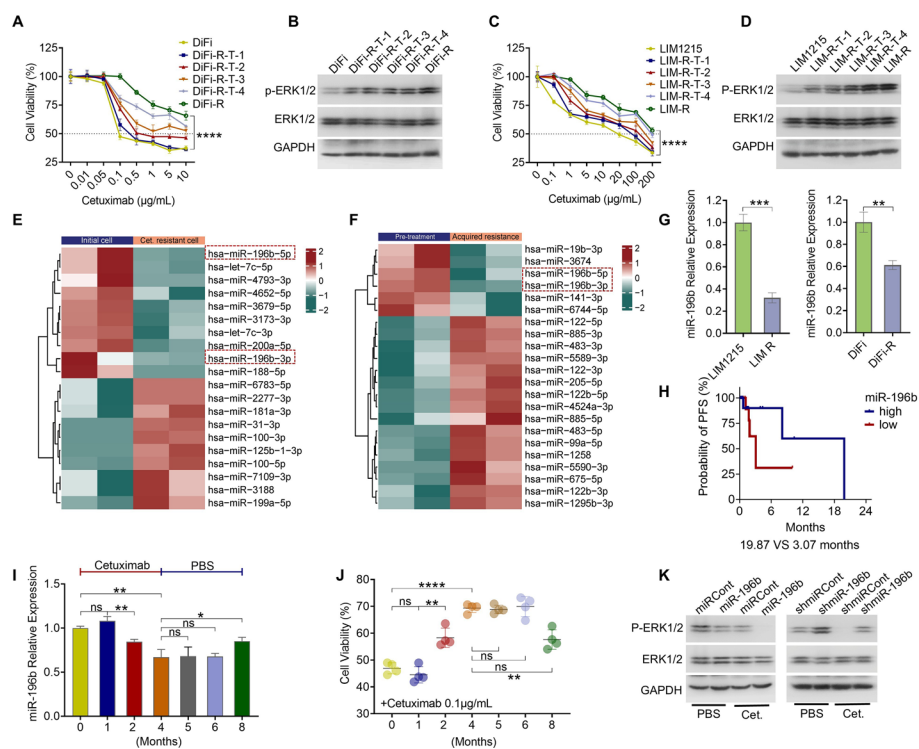


Fig. 1 miR-196b regulates the ERK signaling pathway that changes during cetuximab resistance. **A** Cell viability assay for altered response of DiFi cells to cetuximab during resistance induction (DiFi-R-T-1, induced for 1 month; DiFi-R-T-2, induced for 2 months; DiFi-R-T-3, induced for 3 months; DiFi-R-T-4, induced for 4 months; DiFi-R, induced for more than 6 months). **B** Western blot (WB) analysis of the evolutionary trend of the ERK signaling pathway during the induction of cetuximab resistance in DiFi cells. **C** Cell viability assay for the altered response of LIM1215 cells to cetuximab during resistance induction (LIM-R-T-1, induced for 2 months; LIM-R-T-2, induced for 3 months; LIM-R-T-3, induced for 4 months; LIM-R-T-4, induced for 5 months; LIM-R, induced for more than 6 months). **D** WB analysis of the evolutionary trend of the ERK signaling pathway during the induction of cetuximab resistance in LIM1215 cells. **E** Heat map of differentially expressed genes in the two groups of DiFi cells before and after cetuximab resistance. **F** Heatmap of differentially expressed genes in tumor tissues of two groups of patients before cetuximab treatment and after resistance. **G** Comparison of miR-196b expression levels before and after cetuximab resistance (left, LIM1215; right, DiFi). **H** Comparison of PFS between the miR-196b high-level group ($n = 17$) and the miR-196b low-level group ($n = 17$) in patients with head and neck squamous carcinoma (HNSCC) ($n = 34$) treated with cetuximab. **I** In DiFi cells, miR-196b is downregulated in sustained cetuximab induction and slowly rebounds after withdrawal of the cetuximab. **J** Alterations in the response of DiFi cells to cetuximab during long-term additive induction and withdrawal of the drug (link to I). **K** WB analysis of the effect of miR-196b on the ERK signaling pathway in DiFi cells. * $P < 0.05$, ** $P < 0.01$, *** $P < 0.001$, **** $P < 0.0001$

Supplementary Fig. 1A) before and after the development of drug resistance. Our analysis revealed a significant downregulation of miR-196b following acquired resistance to cetuximab in both cases. These findings were corroborated by qRT-PCR results (Fig. 1G). To preliminarily assess the relationship between miR-196b levels and the prognosis of certain targeted therapies, we analyzed the Cancer Genome Atlas (TCGA) database (<https://portal.gdc.cancer.gov>) and grouped the patients on the basis of the median level of miR-196b. Among patients with head and neck squamous carcinoma (HNSCC) ($n = 34$) treated with cetuximab, those in the miR-196b high-expression group exhibited a longer median progression-free survival (mPFS) of 19.87 months compared with 3.07 months in the low-expression group (Fig. 1H). Similarly, patients with CRC ($n = 41$) treated with bevacizumab and exhibiting high miR-196b expression had a longer mPFS

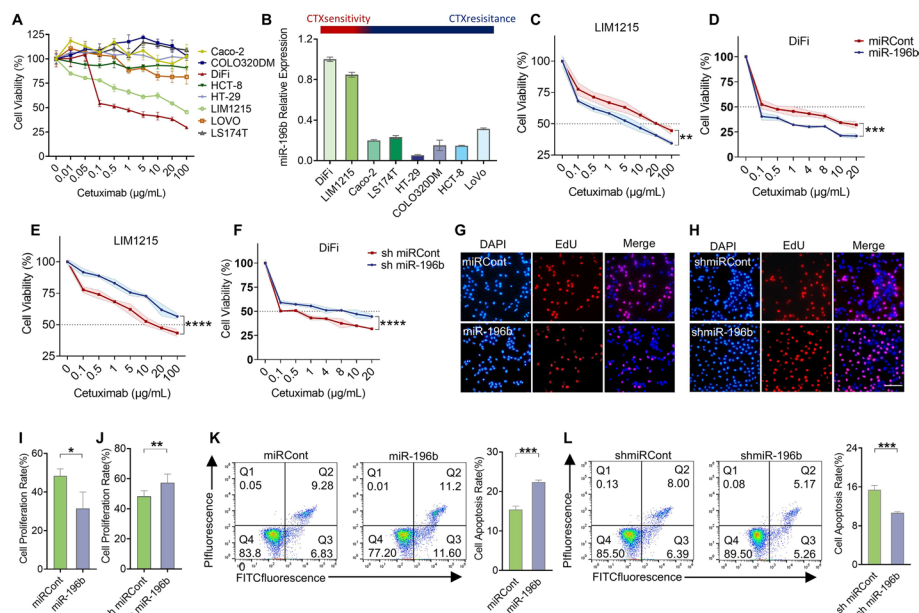


Fig. 2 miR-196b restores CRC cell response to cetuximab. **A** Response of different intestinal cancer cell lines to cetuximab determined by cell viability assay. **B** Determination of miR-196b expression levels in different intestinal cancer cell lines by qRT-PCR. **C** Cell viability assay detects changes in the sensitivity of LIM1215 to cetuximab upon miR-196b overexpression. **D** Cell viability assay detects changes in the sensitivity of DiFi to cetuximab upon miR-196b overexpression. **E** Cell viability assay detects changes in the sensitivity of LIM1215 to cetuximab upon miR-196b silencing. **F** Cell viability assay detects changes in the sensitivity of DiFi to cetuximab upon miR-196b silencing. **G** EdU assay was performed to detect the proliferation rate of LIM1215 cells when cetuximab (20 $\mu\text{g/mL}$) was present and miR-196b was overexpressed. **H** EdU assay was performed to detect the proliferation rate of LIM1215 cells when cetuximab (20 $\mu\text{g/mL}$) was present and miR-196b was silenced. The scale bar is 25 μm . **I** Quantification of LIM1215 cell proliferation upon miR-196b overexpression (link to **G**). **J** Quantification of LIM1215 cell proliferation upon miR-196b silencing (link to **H**). **K** The apoptosis rate of LIM1215 in the presence of cetuximab (20 $\mu\text{g/mL}$) when miR-196b was overexpressed. **L** The apoptosis rate of LIM1215 upon miR-196b silencing in the presence of cetuximab (20 $\mu\text{g/mL}$). * $P < 0.05$, ** $P < 0.01$, *** $P < 0.001$, **** $P < 0.0001$

of 38.33 months versus 12.20 months (Supplementary Material Fig. 1B). Furthermore, an analysis of 616 patients with CRC from the TCGA database indicated a higher percentage of high miR-196b levels in left hemicolon carcinoma (57.1% versus 42.9%, $P = 0.001$) (Supplementary Material Table 1). However, there is no significant correlation between miR-196b level and OS in the CRC/HNSCC population (Supplementary Material Fig. 1C–D). Additionally, we found that under the condition of continuous culture in a medium containing cetuximab, intestinal cancer cells DiFi and LIM1215 showed the first downregulation of miR-196b around 2 months, which became more pronounced with time. However, there was a slow rebound trend within 2–4 months after switching to a normal medium (Fig. 1I and Supplementary Material Fig. 1E). Importantly, on the basis of the results of cell viability assay experiments, we observed that the degree of response to cetuximab in both intestinal cancer cell lines was positively correlated with miR-196b levels (Fig. 1J and Supplementary Material Fig. 1F).

To examine the influence of miR-196b on the activation of the ERK signaling pathway, we established miR-196b overexpression and inhibition cell models in DiFi and LIM1215 cell lines through lentiviral infection (Supplementary Material Fig. 2A–D). Subsequent verification using western blot (WB) analysis confirmed that miR-196b can negatively

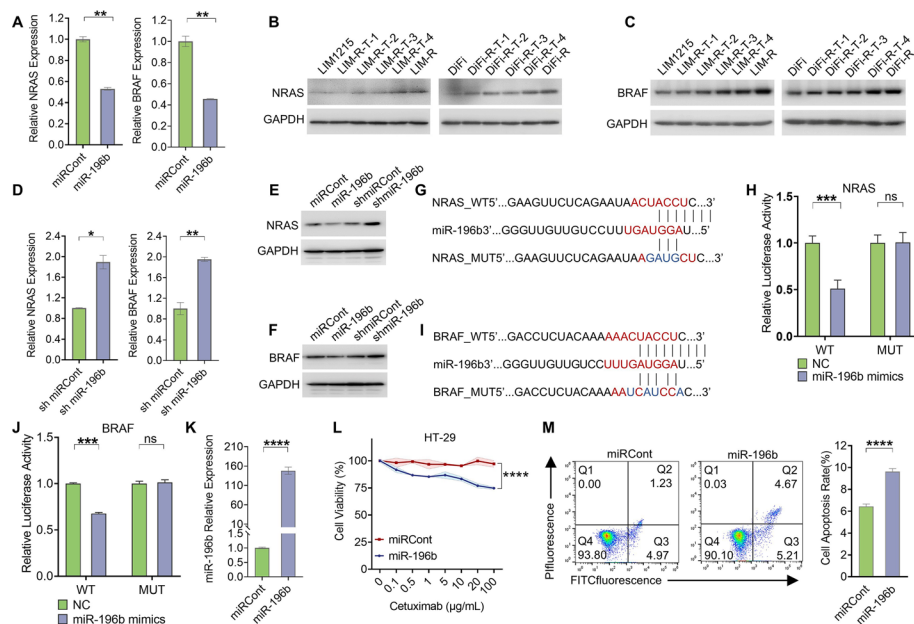


Fig. 3 NRAS and BRAF were direct targets of miR-196b. **A** qPCR detection of NRAS and BRAF expression levels in LIM1215 cell line with miR-196b overexpression. **B** WB analysis of NRAS evolutionary trends during induction of cetuximab resistance (left, LIM1215; right, DiFi). **C** WB analysis of BRAF evolutionary trends during induction of cetuximab resistance (left, LIM1215; right, DiFi). **D** qRT-PCR detection of NRAS and BRAF expression levels in LIM1215 cell line upon miR-196b silencing. **E** WB analysis of changes in NRAS expression in LIM1215 cell line upon miR-196b overexpression or silencing. **F** WB analysis of changes in BRAF expression levels in LIM1215 cell line upon miR-196b overexpression or silencing. **G** Mutations were generated at potential binding sites for miR-196b and the NRAS 3' UTR. **H** Relative luciferase activity of the wild type NRAS 3' UTR or the mutant NRAS 3' UTR at the binding site after transfection of miR-196b mimics in 293 T cells. **I** Mutations were generated at potential binding sites for miR-196b and the BRAF 3' UTR. **J** Relative luciferase activity of the wild-type BRAF 3' UTR or the mutant BRAF 3' UTR at the binding site after transfection of miR-196b mimics in 293 T cells. **K** qRT-PCR validation after overexpression of miR-196b in HT-29. **L** Detection of sensitivity of HT-29 cell line to cetuximab upon miR-196b overexpression by cell viability assay. **M** Detection of apoptosis in HT-29 cell line in the presence of cetuximab (40 μ g/mL) with miR-196b overexpression by flow cytometry. * $P < 0.05$, ** $P < 0.01$, *** $P < 0.001$, **** $P < 0.0001$

regulate the ERK signaling pathway (Fig. 1K, Supplementary Material Fig. 1G). These findings strongly suggest that miR-196b may play a crucial role in mediating resistance to cetuximab.

miR-196b increases the sensitivity of intestinal cancer cells to cetuximab in vitro

We selected eight CRC cell lines for our study: DiFi, LIM1215, Caco-2, LS174 T, HT-29, COLO320DM, HCT-8, and LoVo. Analysis revealed that DiFi and LIM1215 were sensitive to cetuximab, while the remaining cell lines exhibited resistance to the drug (Fig. 2A). The expression level of miR-196b was significantly lower in cetuximab-resistant cells compared with sensitive cell lines, DiFi and LIM1215 (Fig. 2B).

To further investigate the role of miR-196b in CRC, we conducted a series of in vitro experiments. Initially, cell viability assays revealed that overexpression of miR-196b reduced the viability of CRC cells LIM1215 and DiFi under cetuximab treatment, as compared with the control group. This was evidenced by a leftward shift in the IC_{50} trend line, indicating a decrease in IC_{50} (Fig. 2C–D). Conversely, after inhibiting miR-196b

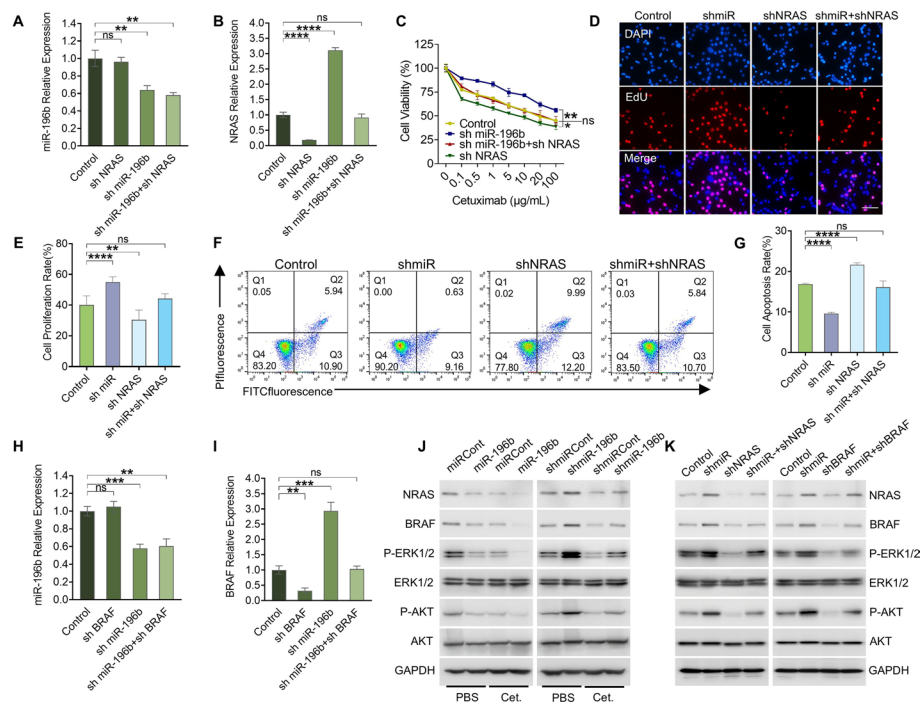


Fig. 4 miR-196b inhibits the activation of ERK and AKT signaling pathways by negatively regulating NRAS and BRAF. **A–B** qRT-PCR was performed to detect the expression of miR-196b **A** and NRAS **B** after knockdown of NRAS, inhibition of miR-196b or simultaneous knockdown of NRAS and miR-196b in the LIM1215 cell. **C** Cell viability assay to detect the sensitivity of LIM1215 cells infected with control, shmiR-196b, or shNRAS lentivirus and coinfecting with shmiR-196b and shNRAS lentivirus to cetuximab. **D–E** EdU analysis (**D**) to detect changes in the proliferation rate (**E**) of LIM1215 cells infected with control, shmiR-196b or shNRAS lentivirus and coinfecting with shmiR-196b and shNRAS lentivirus in the presence of cetuximab (20 μg/mL). The scale bar is 25 μm. **F–G** Flow cytometry (**F**) to detect apoptosis rate (**G**) in LIM1215 cells infected with control, shmiR-196b, or shNRAS lentivirus and coinfecting with shmiR-196b and shNRAS lentivirus in the presence of cetuximab (20 μg/mL). **H–I** qRT-PCR was performed to detect the expression of miR-196b (**H**) and BRAF (**I**) after knockdown of BRAF, inhibition of miR-196b or simultaneous knockdown of BRAF and miR-196b in the LIM1215 cell. **J** WB determination of AKT and ERK signaling pathways in cetuximab (0.1 μg/mL)-treated or untreated DiFi cells in miRCont group, miR-196b group, shCont group, and shmiR-196b group. **K** WB determination of AKT and ERK signaling pathways in DiFi cells in the control group, shmiR-196b group, shNRAS/BRAF group, and shmiR-196b + shNRAS/BRAF group. * $P < 0.05$, ** $P < 0.01$, *** $P < 0.001$, **** $P < 0.0001$

expression, this resulted in increased cell viability and a rightward shift in the IC_{50} trend line, signifying an increase in IC_{50} (Fig. 2E–F). Notably, in the absence of cetuximab, altering miR-196b levels did not affect the proliferation and apoptosis of CRC cells (Supplementary Material Fig. 2E–J). However, in the presence of cetuximab, elevated miR-196b levels inhibited CRC cell proliferation (Fig. 2G, I) and promoted apoptosis (Fig. 2K). By contrast, the silencing of miR-196b accelerated CRC cell proliferation (Fig. 2H, J) and inhibited cell apoptosis (Fig. 2L, Supplementary Material Fig. 2 K–L). Further experiments on drug-resistant cells DiFi-R and LIM-R demonstrated that miR-196b overexpression partially restored the cetuximab response (Supplementary Material Fig. 3A–B), inhibited the proliferation (Supplementary Material Fig. 3C–D), and promoted apoptosis (Supplementary Material Fig. 3E–H) in these resistant cells. Additionally, Transwell and wound healing assay confirmed that miR-196b inhibited CRC cell migration (Supplementary Material Fig. 3I–J) and Supplementary Material Fig. 4).

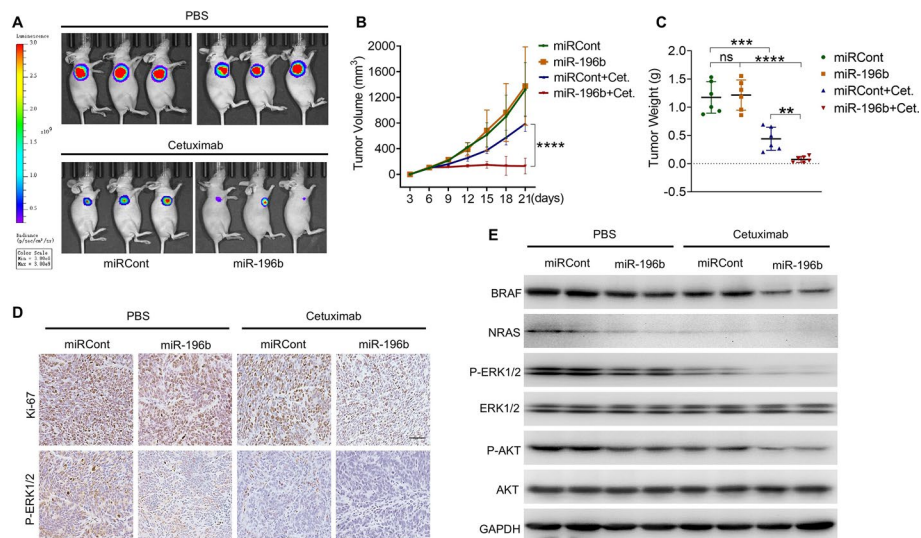


Fig. 5 miR-196b increases sensitivity to cetuximab in vivo. **A** Representative image of cetuximab-treated or untreated tumor xenograft mouse models injected with HT-29 cells infected with control or miR-196b overexpressing lentivirus. **B** Volume curves for xenografts. **C** The final weight of mouse xenografts injected with HT-29 cells. **D** IHC staining for Ki-67 and p-ERK1/2 in xenografts. The scale bar is 25 μ m. **E** Protein expression levels of NRAS, BRAF, p-ERK1/2, and p-AKT were determined by WB in xenografts of cetuximab-treated or untreated HT-29 cells in control and miR-196b groups. ** $P < 0.01$, **** $P < 0.0001$

miR-196b directly targets NRAS and BRAF

To identify potential targets of miR-196b, we made the combined prediction using four miRNA target gene databases, miRBD, Starbase, TargetScan, and DIANA (Supplementary Material Fig. 5A). This initial screening yielded 22 candidate genes potentially linked to cetuximab resistance, which were included in subsequent analyses (Supplementary Material Fig. 5B). In increasing miR-196b expression in CRC cell lines and detecting which of these target genes could be regulated by miR-196b by qRT-PCR (Fig. 3A and Supplementary Fig. 5C–D), we noted two classical genes associated with cetuximab resistance, which were *NRAS* and *BRAF*. Through WB assay of the acquired resistance process of cetuximab in two CRC cell lines, we identified a gradual upregulation trend of *NRAS* and *BRAF* (Fig. 3B–C). The results of qRT-PCR and WB analyses suggested that these key genes are negatively regulated by miR-196b (Fig. 3D–F). To elucidate the interaction between miR-196b and the 3'UTR regions of *NRAS/BRAF*, we performed dual-luciferase reporter assays. Cells were cotransfected with either the pGL3-*NRAS*-3'UTR plasmid, pGL3-*BRAF*-3'UTR plasmid, or pGL3 control plasmid, along with miR-196b mimics or a negative control. The cotransfection with miR-196b mimics significantly reduced the firefly luciferase activity of the *NRAS*-3'UTR and *BRAF*-3'UTR reporter genes, but not the mutant reporter genes (Fig. 3G–J). These findings confirm that *NRAS* and *BRAF* are direct targets of miR-196b.

Previous studies have identified *RAS/RAF* gene mutations as significant drivers of cetuximab resistance [7]. Building on this, we investigated whether miR-196b could influence the responsiveness of *RAS/RAF*-mutated cell lines to cetuximab, particularly after identifying *NRAS* and *BRAF* as targets of miR-196b. Due to the lack of available *NRAS*-mutated CRC cell lines, our experiments focused on the *BRAF V600E*-mutated CRC cell line, HT-29. As we expected, overexpression of miR-196b (Fig. 3K) enhanced

the sensitivity of HT-29 to cetuximab, enabling a response in cells that were previously completely resistant (Fig. 3L). Flow cytometry analysis further revealed that increasing miR-196b expression in the presence of cetuximab elevated the apoptosis rate in HT-29 cells (Fig. 3M). In the CRC cell lines DiFi and LIM1215 without BRAF mutation, miR-196b was also able to regulate BRAF expression and further modulate the sensitivity of CRC cell lines to cetuximab (Supplementary Material Fig. 6).

miR-196b affects CRC cell sensitivity to cetuximab by negatively regulating NRAS and BRAF

The experiments discussed above identified *NRAS* as a downstream mRNA of miR-196b. To further investigate the relationship between *NRAS* and miR-196b in influencing the sensitivity of CRC cells to cetuximab, we employed lentiviral infection to inhibit miR-196b and knock down the expression of *NRAS* in CRC cell lines. The knockdown efficiency was subsequently verified using qRT-PCR experiments. Our findings revealed that co-infection with lentivirus targeting *NRAS* and inhibiting miR-196b resulted in the sustained inhibition of miR-196b (Fig. 4A), while the knockdown efficiency of *NRAS* was lost (Fig. 4B). These results suggest that miR-196b can regulate the expression of *NRAS*, whereas *NRAS* does not influence the expression of miR-196b.

Cell viability assay experiments demonstrated that the knockdown of *NRAS* in CRC cells elevated their sensitivity to cetuximab compared with the control group. Conversely, the inhibition of miR-196b decreased cell sensitivity to cetuximab. However, when both *NRAS* and miR-196b were simultaneously downregulated, there was no significant difference in cetuximab sensitivity compared with the control group (Fig. 4C). In the presence of cetuximab, miR-196b inhibition was found to promote cell proliferation and inhibit apoptosis. Further knockdown of *NRAS* effectively counteracted the effects of miR-196b on proliferation and apoptosis (Fig. 4D–G).

We performed the same experiments on another target gene, *BRAF*, and found that miR-196b could regulate *BRAF* expression, while *BRAF* did not influence miR-196b expression (Fig. 4H–I). The knockdown of *BRAF* counteracted the effects of miR-196b on cetuximab sensitivity (Supplementary Material Fig. 7A), proliferation (Supplementary Material Fig. 7B) and apoptosis (Supplementary Material Fig. 7C) in CRC cells. Additionally, both *NRAS* and *BRAF* were able to eliminate the effect of miR-196b on cell migration (Supplementary Material Fig. 7D–G). These results indicate that *NRAS* and *BRAF* serve as functional targets of miR-196b in CRC cells.

Given that several studies have linked the AKT signaling pathway to cetuximab resistance [15–17], we examined the AKT signaling pathway as well. Western blot analysis revealed that elevating miR-196b expression reduced the phosphorylation levels of AKT and ERK1/2, whereas inhibition of miR-196b led to the opposite effect (Fig. 4J). Furthermore, the knockdown of *NRAS* and *BRAF* counteracted the activation of AKT and ERK signaling pathways caused by miR-196b inhibition (Fig. 4K). These results suggest that miR-196b influences the activation of ERK and AKT signaling pathways by targeting *NRAS* and *BRAF*.

miR-196b restores sensitivity to cetuximab in vivo

To assess the potential of miR-196b in modulating the responsiveness of CRC tumors to cetuximab in vivo, we used two CRC cell lines, HT-29 and LIM1215, for xenograft mouse

experiments. The results suggested no significant difference in tumor size between the miR-196b overexpression group and the control group without cetuximab treatment. However, upon administering cetuximab, the miR-196b overexpression group exhibited a significant reduction in both the size and weight of the HT-29 cell xenografts (Fig. 5A–C). Consistent findings were observed with the LIM1215 cell line, where tumors in the miR-196b overexpression group were notably smaller than those in the control group at various time points following drug administration (Supplementary Material Fig. 8A). Immunohistochemical (IHC) staining of tumor tissues showed decreased antigen Ki67 (Ki-67) positive staining in the miR-196b overexpression group treated with cetuximab. Furthermore, the expression levels of phosphorylated (p)-ERK1/2, p-AKT, NRAS, and BRAF in the tumor tissues of mice were evaluated by IHC and WB analyses. These analyses demonstrated reduced positive staining and expression in the miR-196b group, aligning with our *in vitro* findings (Fig. 5D–E, Supplementary Material Fig. 8B). From the above experimental results, we conclude that miR-196b effectively inhibits CRC tumor growth *in vivo* when combined with cetuximab treatment.

The role of miR-196b as a predictor of cetuximab efficacy in patients with mCRC

Data from 97 patients with CRC treated with cetuximab were analyzed in this study. The patients had a median age of 57 years, ranging from 23 to 77 years, and a mPFS of 13 months. Serum miR-196b level was evaluated by ddPCR. The miR-196b level was divided into high and low groups, with a median value of 31,850 copies/mL; the upper normal limits for carcinoembryonic antigen (CEA) and lactate dehydrogenase (LDH) were set at 5 µg/mL and 245 U/L, respectively. Univariate Cox regression analyses indicated that baseline levels of CEA ($p=0.009$), LDH ($p=0.028$), neutrophil to lymphocyte ratio (NLR) ($p=0.01$), miR-196b ($p<0.001$), and the rate of NLR increase in the first month ($p=0.008$) were significantly associated with PFS (Table 1, Fig. 6A–B and Supplementary Material Fig. 9A–C). We then conducted a multivariate Cox regression analysis incorporating various factors and identified that only the baseline miR-196b levels ($p<0.001$) and the change in NLR within the first month ($p=0.035$) emerged as independent prognostic indicators for PFS. The Kaplan–Meier curve analysis further supported these findings. Specifically, patients with high baseline miR-196b levels exhibited significantly longer PFS compared with those with low levels, with median PFS values of 19.6 months versus 9.8 months, respectively ($P < 0.01$) (Fig. 6A). Additionally, patients whose NLR increased within the first month experienced significantly shorter PFS than those whose NLR decreased, with median PFS values of 14.5 months and 22.7 months, respectively ($P < 0.01$) (Fig. 6B).

On the basis of the results of the multivariate COX regression analysis, we hypothesized that a combined score could more effectively predict the prognosis of patients with mCRC treated with cetuximab. To test this, we calculated the combined scoring of baseline miR-196b levels and NLR growth rate (MNL) score, which incorporates the first month's NLR growth rate and baseline miR-196b levels. Patients were categorized into three groups: the good MNL score group (baseline miR-196b high + NLR decreased within the first month), the intermediate group (baseline miR-196b high + NLR increased within the first month, or baseline miR-196b low + NLR decreased within the

Table 1 Cox regression analysis of PFS in patients with advanced CRC treated with cetuximab

Characteristics	Univariate analysis		Multivariate analysis	
	Hazard ratio (95% confidence intervals, CI)	P-value	Hazard ratio (95% CI)	P-value
Age (years)	1.001 (0.986–1.016)	0.876		
Sex				
Male	Reference			
Female	0.674 (0.431–1.054)	0.084		
Body mass index	0.981 (0.947–1.016)	0.288		
Smoking history				
Never smoke	Reference			
Smoke	0.915 (0.592–1.415)	0.689		
Drinking history				
Never drink	Reference			
Drink	1.471 (0.953–2.272)	0.082		
Metastatic sites				
0–1	Reference			
≥ 2	1.438 (0.946–2.185)	0.089		
Liver metastasis				
Absent	Reference			
Present	1.115 (0.724–1.718)	0.62		
NLR				
< 3	Reference		Reference	
≥ 3	1.820 (1.153–2.874)	0.01	1.831 (1.000–3.355)	0.05
NLR increase rate in the first month	1.148 (1.037–1.271)	0.008	1.119 (1.008–1.243)	0.035
LDH level	1.000 (1.000–1.001)	0.028	1.000 (1.000–1.001)	0.403
Cancer antigen (CA) 19-9 level (U/ml)				
Normal	Reference			
High	1.279 (0.830–1.973)	0.265		
CEA level (µg/ml)				
Normal	Reference		Reference	
High	1.981 (1.182–3.320)	0.009	1.031 (0.532–1.998)	0.929
CEA increase rate in first month	0.991 (0.968–1.015)	0.459		
Cancer antigen (CA) 72-4 level (U/ml)				
Normal	Reference			
High	1.247 (0.812–1.915)	0.312		
miR-196b level (copies/ml)	0.960 (0.945–0.976)	< 0.001	0.956 (0.933–0.980)	< 0.001
miR-196b increase rate in first month	0.882 (0.108–7.177)	0.907		

NLR neutrophil to lymphocyte ratio; LDH lactate dehydrogenase

first month), and the poor MNL score group (baseline miR-196b low + NLR increased within the first month). Our analysis revealed that patients in the good MNL score group had significantly longer PFS compared with those in the intermediate/poor score group, with mPFS of 22.7 months versus 10.7 months, respectively ($P < 0.01$). We introduced the concept of Δ mPFS to denote the difference in mPFS between groups. For example, the difference (Δ mPFS is the mPFS of the miR-196b high group minus the mPFS of the miR-196b low group) is used to assess the predictive effect of miR-196b levels on mPFS. A larger Δ mPFS implies a more significant predictive value. Compared with the baseline miR-196b-predicted PFS (Δ mPFS = 9.8 months) and the NLR increase rate in

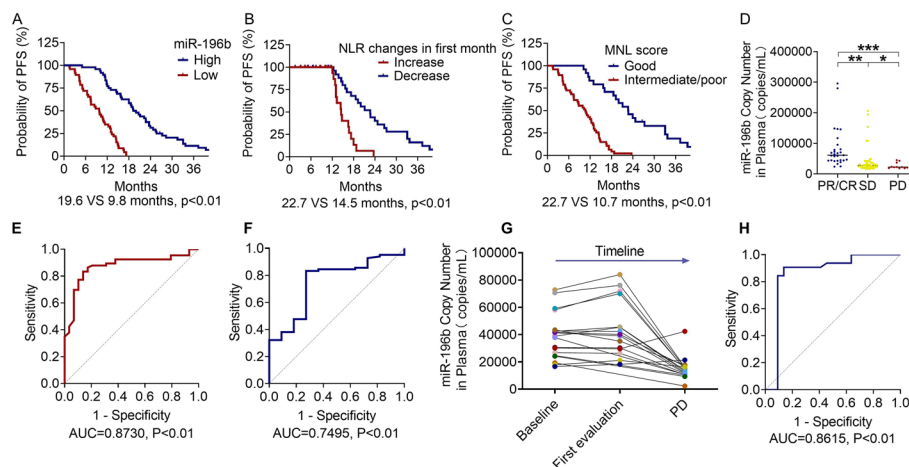


Fig. 6 miR-196b can be used to predict the efficacy of cetuximab in patients with CRC ($n = 97$). **A** Comparison of PFS between the high-level ($n = 49$) or low-level ($n = 48$) miR-196b groups in patients with CRC treated with cetuximab. **B** Comparison of PFS between NLR first-month-rise ($n = 24$) and first-month-fall ($n = 73$) groups in patients with CRC treated with cetuximab. **C** Comparison of PFS between the good combined scoring of baseline miR-196b levels and NLR growth rate (MNL) score ($n = 25$) or intermediate/poor group ($n = 72$) in patients with CRC treated with cetuximab. **D** Absolute quantification of baseline copy number of miR-196b in plasma from patients with partial response (PR)/complete response (CR), stable disease (SD), and progressive disease (PD) by droplet digital PCR. **E–F** ROC curves for baseline miR-196b levels to predict PR **E** or PD **F** in the first efficacy evaluation. **G** Dynamic monitoring of patient efficacy of cetuximab treatment using miR-196b levels. **H** ROC curves were used to determine the magnitude of miR-196b decline when efficacy was assessed as PD. * $P < 0.05$, ** $P < 0.01$, *** $P < 0.001$

the first month (Δ mPFS = 8.2 months), the difference of the MNL coscoring Δ mPFS of 12 months was larger, i.e., the difference of the median survival between the good MNL coscoring and the intermediate/poor score was nearly 1 year. This indicates that the MNL combined score is a good indicator for predicting PFS in patients with mCRC using cetuximab (Fig. 6C).

We collected the baseline levels of several metrics, including miR-196b, tumor markers cancer antigen (CA) 19-9, CA 72-4, CEA, and NLR, to evaluate the association with the initial efficacy of cetuximab treatment. Our findings indicate a strong correlation between baseline miR-196b levels and the initial efficacy in patients with mCRC treated with cetuximab. Specifically, patients exhibiting high miR-196b levels were more likely to have a partial response (PR) or complete response (CR) during the first efficacy evaluation. In contrast, those with low miR-196b levels were more prone to experience progressive disease (PD) at the initial assessment (Fig. 6D). Conversely, baseline levels of CA 19-9, CA 72-4, CEA, and NLR did not show a significant correlation with first efficacy outcomes in patients with mCRC undergoing cetuximab treatment (Supplementary Fig. 9D–G).

After establishing that baseline miR-196b levels correlate with the initial response to cetuximab, we then employed ROC curve analysis to determine the cutoff value for predicting the PR at the first efficacy evaluation. The analysis revealed that the maximum Youden index was 0.695 at a cutoff value of 42,262.5 copies/mL, with a sensitivity of 86.2%, specificity of 83.3%, and an area under the curve (AUC) of 0.873 (95% confidence intervals, CI 0.7970–0.9491), $P < 0.01$. This indicates that patients with baseline miR-196b levels above 42,262.5 copies/mL are more likely to achieve PR at the first

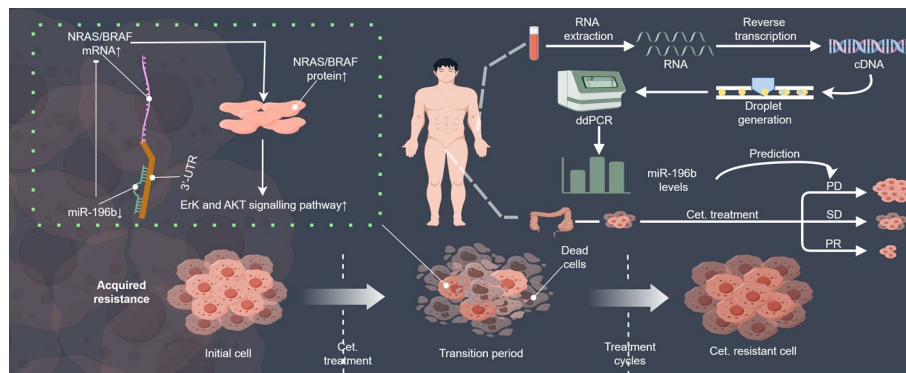


Fig. 7 Graphical Abstract. (1) During the process of acquired resistance to cetuximab in CRC cells, alterations in sensitivity are accompanied by significant changes in multiple cellular functions, including proliferation, apoptosis, and migration. (2) During acquired resistance to cetuximab in CRC cells, miR-196b expression was decreased, thus leading to the elevation of NRAS and BRAF, and ERK and AKT signaling pathways were activated. (3) miR-196b serves as a predictive and monitoring biomarker for assessing changes in patients' conditions

evaluation (Fig. 6E). Similarly, we investigated the cutoff value for predicting PD using ROC curve analysis. The maximum Yoden index of 0.561 was observed at a cutoff value of 23,800.0copies/mL, with a sensitivity of 83.3%, specificity of 72.7%, and an AUC of 0.7495 (95% CI 0.6034–0.8955), $P < 0.01$. This suggests that patients with baseline miR-196b levels below 23,800.0 copies/mL are more likely to experience PD at the first evaluation (Fig. 6F).

To explore whether miR-196b levels can serve as a dynamic marker for monitoring the efficacy of cetuximab in patients with mCRC, we conducted a longitudinal study involving 19 patients, measuring miR-196b levels in their plasma. Our analysis found that during long-term cetuximab treatment, most of the patients that developed PD exhibited a noticeable decline in miR-196b levels concurrent with disease progression (Fig. 6G). Through ROC curve analysis, we determined that the maximum Yoden index of 0.770 was reached at a 26.8% decrease in miR-196b levels from baseline, with a sensitivity of 90.6% and a specificity of 86.4% under this condition. The AUC was 0.8615 (95% CI 0.7356–0.9874), with a significance of $P < 0.01$. This suggests that a reduction in blood miR-196b levels exceeding 26.8% from baseline may indicate disease progression (Fig. 6H). Therefore, miR-196b can potentially be utilized to dynamically monitor cetuximab efficacy in patients with mCRC.

Discussion

Current research on the relationship between ncRNA and resistance to anti-EGFR therapy remains sparse and necessitates further investigation. Notably, ncRNAs can exhibit diverse or even contradictory roles across different tumor types. For example, miR-196b functions as a tumor suppressor in CRC, where its high expression inhibits the migration of CRC cells and was associated with a good prognosis for patients [18]. Conversely, in lung cancer, miR-196b facilitates the proliferation of cancer cells [19]. By analyzing the TCGA database, we found a higher percentage of miR-196b high expression in left hemicolon cancer. A recent study by Solar Vasconcelos et al. showed a better prognosis with cetuximab in left hemicolon cancer [20], which we presumed may be related

to miR-196b overexpression in left hemicolon cancer. Small RNA sequence analysis revealed that miR-196b was significantly downregulated both in cetuximab-resistant CRC cell models and in drug-resistant tissues from patients with mCRC, suggesting a potential link between miR-196b downregulation and cetuximab resistance development. By analyzing the TCGA database, we found that patients with HNSCC with high miR-196b expression had longer PFS with cetuximab treatment (19.87 m versus 3.07 m). The collection of patients with CRC using cetuximab in the TCGA database was too small for statistical analysis. Bevacizumab targets vascular endothelial growth factor (VEGF), while cetuximab targets EGFR, and there are common downstream signaling pathways between them, such as ERK1/2 and PI3 K/AKT signaling pathways (Supplementary Material Fig. 11). Therefore, we evaluated the data of patients with CRC treated with bevacizumab in the TCGA database. We found similar conclusions as HNSCC, in that high expression of miR-196b is associated with a better prognosis with targeted therapies. In vitro experiments demonstrated that miR-196b overexpression, in the presence of cetuximab, inhibited CRC cell proliferation, promoted apoptosis, and reduced the IC₅₀ of cetuximab. Conversely, silencing miR-196b produced the opposite effects. Regardless of the presence or absence of cetuximab, overexpression of miR-196b can slow down the migration of CRC cells, which is consistent with the previous study by Stiegelbauer et al. [18].

Numerous studies have established a strong correlation between RAS/RAF pathways and resistance to cetuximab [21, 22]. Our research corroborates these findings, demonstrating that NRAS and BRAF expression levels increase progressively during the simulated drug resistance process. Importantly, we found that miR-196b was able to negatively regulate these two critical targets, thus making tumor cells more sensitive to cetuximab. NRAS/BRAF was upregulated upon miR-196b silencing, thereby leading to the activation of the ERK signaling pathway and the PI3 K/AKT signaling pathway and, ultimately, cetuximab resistance. miR-196b acts mainly through NRAS/BRAF, and further inhibition of NRAS/BRAF expression on the basis of miR-196b silencing would counteract the effects of miR-196b silencing. Notably, in the HT-29 cell line, a natural drug-resistant cell line with *BRAF V600E* mutation, miR-196b overexpression was also able to partially restore its sensitivity to cetuximab independent of the BRAF mutation. Therefore, we speculate that as long as the binding site of miR-196b to its target gene is not at the mutation site, it can successfully regulate its target gene. However, since there were no NRAS-mutated CRC cell lines available, we were unable to validate the same for NRAS-mutated CRC cells. Although there are effective regimens for maintaining the efficacy of cetuximab in patients with CRC with *BRAF V600E* mutation in clinical treatment [23, 24], there is currently no drug that can target both NRAS and BRAF. Owing to the significant individualized differences among patients with tumor, not all patients treated with cetuximab had only one mechanism of resistance, a BRAF mutation; several patients' acquired resistance was due to the emergence of a NRAS mutation, and there was no available NRAS inhibitor in CRC treatment. Therefore, miR-196b was a very promising sensitizing factor for cetuximab.

Numerous studies have investigated the resistance mechanisms of anti-EGFR monoclonal antibodies, with particular focus on the ERK and AKT signaling pathways [7, 25, 26]. Specifically, cotargeting the EGFR and PI3 K/AKT pathway or the MAPK/ERK

pathway can produce a synergistic effect of drugs, thus restoring sensitivity to sensitivity to EGFR inhibitors [27, 28]. In our study, miR-196b was found to be able to downregulate the activities of both ERK and AKT signaling pathways, and NRAS and BRAF were the bridges of communication between miR-196b and ERK and AKT signaling pathways. The ERK signaling pathway is recognized as the downstream signaling pathway of RAS/RAF. Further studies found that miR-196b was upregulated after the inhibition of the ERK signaling pathway using U0126, a result that suggests that there appears to be a negative correlation between the ERK signaling pathway and miR-196b, of which key regulators have been mentioned in several previous studies (Supplementary Material Fig. 10 F). Sun et al. found that the expression of METTL3 was higher upon ERK activation. Inhibition of ERK increased the ubiquitination of METTL3, suggesting that ERK activation stabilizes the protein by decreasing METTL3 ubiquitination [29], while another study indicated that miR-196b maturation is inhibited and expression decreases upon increased METTL3 expression [30]. On the basis of the findings of these two studies, we verified METTL3, which may play a key role, and determined that the activation of the ERK signaling pathway could upregulate the expression of METTL3 and lead to the downregulation of miR-196b. Combined with previous studies, we confirmed that miR-196b is regulated by the activation of the ERK signaling pathway and that METTL3 plays a key role in it (Supplementary Material Fig. 10 A–F). Therefore, there is a critical signaling loop in the cetuximab resistance process, and downregulation of miR-196b can upregulate the expression of target genes NRAS and BRAF, thus activating the ERK signaling pathway. The activation of the ERK signaling pathway can upregulate METTL3 expression and thus downregulate miR-196b expression (Supplementary Material Fig. 10G). A recent study summarized the crosstalk between several signaling pathways, including the interaction between the ERK signaling pathway and the AKT signaling pathway. The ERK signaling pathway can activate its downstream STAT3, which is the upstream activator of AKT, and thus can activate the AKT signaling pathway [31]. This also explained why NRAS and BRAF, as key components of the RAS/RAF/MEK/ERK signaling pathway, can affect the activation of the AKT signaling pathway. Afterward, we reconfirmed the above conclusions by conducting *in vivo* experiments in nude mice and performing IHC and WB tests on tumor tissues.

Regarding clinical treatment, we collected clinicopathologic data from patients with advanced CRC treated with cetuximab at the Chinese PLA General Hospital as well as blood samples from multiple cycles to test miR-196b levels. Univariate analysis suggested that patients' baseline CEA, LDH, NLR, miR-196b levels, and changes in NLR within the first month of treatment were all associated with patients' PFS after treatment with cetuximab. Several previous studies have demonstrated the predictive value of NLR for prognosis in the treatment of a variety of cancers [32]. Similar conclusions were obtained in our study. Further multivariate analysis showed that the change of NLR within the first month was an independent prognostic factor for PFS. In addition, we found that miR-196b, which we focused on, was also an independent prognostic factor for PFS. The mPFS was significantly longer in the baseline miR-196b high-level group compared with the low-level group, at 19.6 and 9.8 months, respectively ($P < 0.01$). On the basis of the results of the multifactorial analysis, we hypothesized that a combined score of the two could better predict the prognosis of advanced patients with CRC treated with cetuximab. Therefore,

we first proposed to calculate the MNL combined score on the basis of the changes in NLR within the first month of treatment and the baseline level of miR-196b. The analysis suggests that the MNL joint score can better predict the prognosis of patients with CRC treated with cetuximab than the change in NLR within the first month of treatment or the baseline level of miR-196b. This prognostic indicator can be inferred from patients' blood test results, which are easily reproducible and widely available.

In addition, this study also found that baseline miR-196b level can be used to predict the initial efficacy of cetuximab. The ROC curve analysis results showed that when the baseline miR-196b level was higher than 42,262.5 copies/mL, the patients were more likely to achieve PR in the first evaluation. When the baseline miR-196b level was lower than 23,800.0 copies/mL, patients were more likely to be evaluated for PD for the first time. However, in our study, although the baseline CEA level was associated with PFS in patients with CRC treated with cetuximab, it could not be used to predict the initial efficacy of cetuximab. CEA is a relatively broad-spectrum tumor marker that is expressed in many epithelial tumors and is mainly used to evaluate the changes in tumor load caused by recurrent metastasis [33]; however, it cannot directly affect the efficacy of cetuximab. However, miR-196b is different. In our study, basic experiments have confirmed that it can promote the efficacy of cetuximab and is a favorable sensitizer. Therefore, this also explains why miR-196b can be used to predict the first efficacy of cetuximab.

More importantly, the study found that miR-196b can be used to dynamically monitor the efficacy of cetuximab in patients with CRC. When the miR-196b level of the patient's blood decreases by more than 26.8% compared with the baseline, it indicates that the patient's disease may be progressing, which needs to be paid attention to by clinicians. In our clinical work, imaging examinations are generally performed every 6–8 weeks, but routine laboratory tests are performed after each treatment (approximately once every 2–4 weeks). Therefore, changes in miR-196b levels obtained by blood tests can help us realize the progression of patients' disease during cetuximab treatment 2–6 weeks in advance, which has clinical application value.

Conclusions

In conclusion, our study demonstrated that miR-196b plays a crucial role in modulating the response of CRC to cetuximab by negatively regulating *NRAS* and *BRAF*, which leads to the downregulation of ERK and AKT signaling pathway activities. Furthermore, miR-196b serves as a robust predictive and monitoring biomarker for assessing changes in patients' conditions (Fig. 7). This capability aids clinicians in identifying patients with CRC who are most likely to benefit from cetuximab treatment, thereby facilitating individualized and precise therapeutic strategies.

Abbreviations

CRC	Colorectal cancer
miRNA	MicroRNA
ddPCR	Droplet digital polymerase chain reaction
mCRC	Metastatic colorectal cancer
ncRNA	Non-coding RNA
IC ₅₀	Half maximal inhibitory concentration
NLR	Neutrophil to lymphocyte ratio
HNSCC	Head and neck squamous carcinoma
PFS	Progression-free survival
OS	Overall survival

mPFS	Median progression-free survival
WB	Western blot
IHC	Immunohistochemical
LDH	Lactate dehydrogenase
ROC	Receiver operating characteristic
PR	Partial response
CR	Complete response
PD	Progressive disease
AUC	Area under the curve

Supplementary Information

The online version contains supplementary material available at <https://doi.org/10.1186/s11658-025-00740-8>.

Additional file 1.

Acknowledgements

The authors thank the Figdraw platform for visualization.

Author contributions

Y.W., G.D., Z.W., and S.C. conceived and designed the study. Y.W., S.C., G.D., Z.W., Z.T., Y.L., F.P., and X.W. conducted literature retrieval and developed the implementation plan. S.C., Z.T., and Y.L. performed the experiments. S.C., Z.T., Y.L., F.P., and X.L. analyzed and interpreted the data. Y.W., S.C., G.D., Z.W., and Z.T. wrote, reviewed, and revised the manuscript. Y.C., W.M., Y.L., and L.H. provided administrative and technical support. Y.L. and M.G. provided material support. Y.W., G.D., and Z.W. were responsible for study supervision. All authors reviewed and approved the final manuscript.

Funding

This work was supported by the National Key Research and Development Program of China (nos. 2019YFA0903800 and 2022YFC3600100), the National Natural Science Foundation of China (nos. 82002474 and 82272643) and the Natural Science Foundation of Beijing Municipal (no. 7222176).

Availability of data and materials

All data for this study are available from the corresponding author on reasonable request.

Declarations

Ethics approval and consent to participate

For patients' tissue, blood samples, and data, the protocol was approved by the Ethics Committee of Chinese PLA General Hospital (approval no. KY2023-6-42-1, date: 28 June 2023), in accordance with the Declaration of Helsinki and with informed consent from all patients. All animal experiments were approved by the Animal Welfare Ethics Committee of the Beijing Institute of Biotechnology (approval no. IACUC-DWZX-2023-052, date: 2 November 2023) and in accordance with the Basel Declaration. The Animal Welfare Ethics Committee of the Beijing Institute of Biotechnology strictly adheres to the principles and guidelines established by the International Council for Laboratory Animal Science (ICLAS) to ensure that our animal research meets international ethical standards.

Consent for publication

Not applicable.

Competing interests

The authors declare no competing interests.

Received: 8 January 2025 Accepted: 6 May 2025

Published online: 25 May 2025

References

1. Bray F, Laversanne M, Sung H, Ferlay J, Siegel RL, Soerjomataram I, et al. Global cancer statistics 2022: GLOBOCAN estimates of incidence and mortality worldwide for 36 cancers in 185 countries. *CA Cancer J Clin*. 2024;74:229–63.
2. Bando H, Ohtsu A, Yoshino T. Therapeutic landscape and future direction of metastatic colorectal cancer. *Nat Rev Gastroenterol Hepatol*. 2023;20:306–22.
3. Khan KH, Cunningham D, Werner B, Vlachogiannis G, Spiteri I, Heide T, et al. Longitudinal liquid biopsy and mathematical modeling of clonal evolution forecast time to treatment failure in the PROSPECT-C phase II colorectal cancer clinical trial. *Cancer Discov*. 2018;8:1270–85.
4. Tan Z, Gao L, Wang Y, Yin H, Xi Y, Wu X, et al. PRSS contributes to cetuximab resistance in colorectal cancer. *Sci Adv*. 2020;6:eaax5576.
5. Bardelli A, Janne PA. The road to resistance: EGFR mutation and cetuximab. *Nat Med*. 2012;18:199–200.
6. Klomp JA, Klomp JE, Stalnecker CA, Bryant KL, Edwards AC, Drizyte-Miller K, et al. Defining the KRAS- and ERK-dependent transcriptome in KRAS-mutant cancers. *Science*. 2024;384:eadk0775.

7. Zhou J, Ji Q, Li Q. Resistance to anti-EGFR therapies in metastatic colorectal cancer: underlying mechanisms and reversal strategies. *J Exp Clin Cancer Res.* 2021;40:328.
8. Wei S, Hu W, Feng J, Geng Y. Promotion or remission: a role of noncoding RNAs in colorectal cancer resistance to anti-EGFR therapy. *Cell Commun Signal.* 2022;20:150.
9. Aparicio-Puerta E, Hirsch P, Schmartz GP, Kern F, Fehlmann T, Keller A. miEAA 2023: updates, new functional micro-RNA sets and improved enrichment visualizations. *Nucleic Acids Res.* 2023;51:W319–25.
10. Dogra P, Shinglot V, Ruiz-Ramírez J, Cave J, Butner JD, Schiavone C, et al. Translational modeling-based evidence for enhanced efficacy of standard-of-care drugs in combination with anti-microRNA-155 in non-small-cell lung cancer. *Mol Cancer.* 2024;23:156.
11. Zhu Y, Yu F, Jiao Y, Feng J, Tang W, Yao H, et al. Expression of concern: reduced miR-128 in breast tumor-initiating cells induces chemotherapeutic resistance via Bmi-1 and ABCG5. *Clin Cancer Res.* 2024;30:2847.
12. Pucci P, Lee LC, Han M, Matthews JD, Jahangiri L, Schleder M, et al. Targeting NRAS via miR-1304-5p or farnesyltransferase inhibition confers sensitivity to ALK inhibitors in ALK-mutant neuroblastoma. *Nat Commun.* 2024;15:3422.
13. Klomp JE, Diehl JN, Klomp JA, Edwards AC, Yang R, Morales AJ, et al. Determining the ERK-regulated phosphoproteome driving KRAS-mutant cancer. *Science.* 2024;384:eadk0850.
14. Chen S, Tan Z, Wu X, Lin Y, Li X, Cui Y, et al. Single-cell sequencing analysis reveals cetuximab resistance mechanism and salvage strategy in colorectal cancer. *Clin Transl Med.* 2025;15: e70151.
15. Cruz-Duarte R, Rebelo de Almeida C, Negrão M, Fernandes A, Borralho P, Sobral D, et al. Predictive and therapeutic implications of a novel PLCγ1/SHP2-driven mechanism of cetuximab resistance in metastatic colorectal cancer. *Clin Cancer Res.* 2022;28:1203–16.
16. Yamada T, Takeuchi S, Kita K, Bando H, Nakamura T, Matsumoto K, et al. Hepatocyte growth factor induces resistance to anti-epidermal growth factor receptor antibody in lung cancer. *J Thorac Oncol.* 2012;7:272–80.
17. Han Y, Peng Y, Fu Y, Cai C, Guo C, Liu S, et al. MLH1 deficiency induces cetuximab resistance in colon cancer via her-2/PI3K/AKT signaling. *Adv Sci.* 2020;7:2000112.
18. Stiegelbauer V, Vychytilova-Faltejskova P, Karbiener M, Pehserl AM, Reicher A, Resel M, et al. miR-196b-5p regulates colorectal cancer cell migration and metastases through interaction with HOXB7 and GALNT5. *Clin Cancer Res.* 2017;23:5255–66.
19. Liang G, Meng W, Huang X, Zhu W, Yin C, Wang C, et al. miR-196b-5p-mediated downregulation of TSPAN12 and GATA6 promotes tumor progression in non-small cell lung cancer. *Proc Natl Acad Sci USA.* 2020;117:4347–57.
20. Solar Vasconcelos JP, Chen N, Titmuss E, Tu D, Brule SY, Goodwin R, et al. Transverse colon primary tumor location as a biomarker in metastatic colorectal cancer: a pooled analysis of CCTG/AGITG CO.17 and CO.20 randomized clinical trials. *Clin Cancer Res.* 2024;30:1121–30.
21. Yao Y, Wang Y, Chen L, Tian Z, Yang G, Wang R, et al. Clinical utility of PDX cohorts to reveal biomarkers of intrinsic resistance and clonal architecture changes underlying acquired resistance to cetuximab in HNSCC. *Signal Transduct Target Ther.* 2022;7:73.
22. Woolston A, Khan K, Spain G, Barber LJ, Griffiths B, Gonzalez-Exposito R, et al. Genomic and transcriptomic determinants of therapy resistance and immune landscape evolution during anti-EGFR treatment in colorectal cancer. *Cancer Cell.* 2019;36:35–50.e9.
23. Napolitano S, Woods M, Lee HM, De Falco V, Martini G, Della Corte CM, et al. Antitumor efficacy of dual blockade with encorafenib + cetuximab in combination with chemotherapy in human BRAFV600E-mutant colorectal cancer. *Clin Cancer Res.* 2023;29:2299–309.
24. Van Cutsem E, Taieb J, Yaeger R, Yoshino T, Grothey A, Maiello E, et al. ANCHOR CRC: results from a single-arm, phase II study of encorafenib plus binimetinib and cetuximab in previously untreated BRAF(V600E)-mutant metastatic colorectal cancer. *J Clin Oncol.* 2023;41:2628–37.
25. Martini G, Ciardiello D, Vitiello PP, Napolitano S, Cardone C, Cuomo A, et al. Resistance to anti-epidermal growth factor receptor in metastatic colorectal cancer: what does still need to be addressed? *Cancer Treat Rev.* 2020;86: 102023.
26. Ye LF, Huang ZY, Chen XX, Chen ZG, Wu SX, Ren C, et al. Monitoring tumour resistance to the BRAF inhibitor combination regimen in colorectal cancer patients via circulating tumour DNA. *Drug Resist Updat.* 2022;65: 100883.
27. Zaryouh H, De Pauw I, Baysal H, Peeters M, Vermorken JB, Lardon F, et al. Recent insights in the PI3K/Akt pathway as a promising therapeutic target in combination with EGFR-targeting agents to treat head and neck squamous cell carcinoma. *Med Res Rev.* 2022;42:112–55.
28. Li K, Wu JL, Qin B, Fan Z, Tang Q, Lu W, et al. ILF3 is a substrate of SPOP for regulating serine biosynthesis in colorectal cancer. *Cell Res.* 2020;30:163–78.
29. Sun HL, Zhu AC, Gao Y, Terajima H, Fei Q, Liu S, et al. Stabilization of ERK-phosphorylated METTL3 by USP5 increases m(6)A methylation. *Mol Cell.* 2020;80:633–47.e7.
30. Han X, Li G, Yang H, Zhang C, Cao Y, Wang N, et al. METTL3 promotes osteo/odontogenic differentiation of stem cells by inhibiting miR-196b-5p maturation. *Stem Cells Int.* 2023;2023:8992284.
31. Jin Y, Liu M, Sa R, Fu H, Cheng L, Chen L. Mouse models of thyroid cancer: bridging pathogenesis and novel therapeutics. *Cancer Lett.* 2020;469:35–53.
32. Xie H, Wei L, Ruan G, Zhang H, Shi J, Lin S, et al. AWGC2023 cachexia consensus as a valuable tool for predicting prognosis and burden in Chinese patients with cancer. *J Cachexia Sarcopenia Muscle.* 2024;15:2084–93.
33. Sørensen CG, Karlsson WK, Pommegaard HC, Burcharth J, Rosenberg J. The diagnostic accuracy of carcinoembryonic antigen to detect colorectal cancer recurrence—A systematic review. *Int J Surg.* 2016;25:134–44.

Publisher's Note

Springer Nature remains neutral with regard to jurisdictional claims in published maps and institutional affiliations.